

EFFECT OF COVER GAS PRESSURES UP TO 4 ATMOSPHERES ON
ACCELERATED CAVITATION DAMAGE IN SODIUM

by S. G. Young and J. R. Johnston

CONTENTS (For review copy only)

E-3860

	Page
SUMMARY	1
INTRODUCTION	2
MATERIALS, APPARATUS AND PROCEDURE	4
Materials	4
Accelerated Cavitation Damage Test Facility	4
Test Conditions	5
Test Procedure	5
CAVITATION DAMAGE RESULTS	6
Volume Loss and Volume Loss Rate	6
Relation Between Steady State Volume Loss Rate and Pressure	8
Metallography	10
Comparison of Accelerated Cavitation Damage and Pump Impeller Test Results	12
SUMMARY OF RESULTS	13
REFERENCES	15

N68-22341

FACILITY FORM 602	_____ (ACCESSION NUMBER)	_____ (THRU)
	39 (PAGES)	1 (CODE)
	TMX-61065 (NASA CR OR TMX OR AD NUMBER)	17 (CATEGORY)

TECHNICAL NOTE

EFFECT OF COVER GAS PRESSURES UP TO 4 ATMOSPHERES ON
ACCELERATED CAVITATION DAMAGE IN SODIUM

by S. G. Young and J. R. Johnston

ABSTRACT

Increasing cover gas pressures up to 4 atmospheres significantly increased cavitation damage to three materials; AISI type 316 stainless steel, L-605, and Stellite 6B in a vibratory test apparatus. Specimens were tested in sodium at 800° F (700° K). When volume loss was normalized to include only heavily damaged portions of specimens, damage increased exponentially with pressure for all materials. Materials were ranked with respect to cavitation damage resistance in the same order at high pressures as at low pressures. Metallographic studies were conducted to determine the nature of damage to the materials.

EFFECT OF COVER GAS PRESSURES UP TO 4 ATMOSPHERES ON ACCELERATED CAVITATION DAMAGE IN SODIUM

by S. G. Young and J. R. Johnston

Lewis Research Center

SUMMARY

An investigation was made to study the effect of pressure on the resistance to cavitation damage of materials under consideration for components of liquid metal power conversion systems. A vibratory apparatus was used to subject three materials, AISI 316 stainless steel, L-605, and Stellite 6B to accelerated cavitation damage in sodium at 800° F (700° K). Argon cover gas was used to maintain pressures up to 4 atmospheres during test. Volume loss and volume loss rate measurements were used to compare the effects of pressure on the degree of damage. Metallographic studies were conducted to determine the nature of damage.

Increasing cover gas pressure significantly increased cavitation damage to all materials for all exposure times. The materials ranked in the same order with respect to resistance to cavitation damage at all pressures; Stellite 6B was most resistant, L-605 intermediate and 316 stainless steel, least resistant. The steady state volume loss rate based on total specimen area increased linearly with cover gas pressure. When the volume loss rate data were normalized to include only the heavily damaged area of the specimens, the steady state volume loss rate increased exponentially with pressure. Metallographic examination of axially sectioned specimens revealed undercutting and transgranular

cracking as well as subsurface deformation for all materials.

INTRODUCTION

Components of advanced space power systems have shown cavitation damage in the form of pitting and surface erosion when tested for several hundred hours in liquid metal loops (ref. 1-3). Proposed power systems must function for 10 000 hours or longer and it is important to determine the resistance to cavitation damage of candidate materials in advance of service. Studies are being made of the resistance of materials to cavitation attack in liquid metals using accelerated types of laboratory tests, and considerable data describing material performance under cavitating conditions have been obtained. Some of the more recent of these investigations are described in references 4 to 6.

Extensive research is also being conducted to investigate the mechanism of cavitation and how the process causes material damage. Some of this work is presented in references 7 to 9. The process can briefly be described as follows: When local pressures in fluids fall below the fluid vapor pressure, cavities form. The pressure within a cavity or cavitation bubble is believed to be near the vapor pressure of the fluid (ref. 10). When these cavities are then subjected to regions of higher pressure, they collapse with high velocity. If the collapse occurs on a solid surface such as a metal, localized high pressures can be transmitted to the surface resulting in severe damage.

In power conversion systems, fluid pressures can vary, depending on the operating conditions, from near the fluid vapor pressures at the pump inlet to hundreds of pounds per square inch at the pump outlet.

Some early studies were made to determine the effect of higher pressures on accelerated cavitation damage in water (ref. 11). These studies showed that increasing pressure up to 2 atmospheres increased cavitation damage, but higher pressures up to 4 atmospheres suppressed damage. Most other investigations of accelerated cavitation damage, and particularly those using fluids other than water, have been performed at ambient pressures approximately equal to atmospheric pressure.

Greatly simplified, the difference between the local ambient pressure and the vapor pressure may be considered to be the net pressure or head available to collapse an existing cavitation bubble. The greater this pressure difference, or driving force, the higher will be the velocity of the fluid bubble wall impacting the surface. As a result, the impact force will be higher and the resulting cavitation damage will be greater. Isolating the pressure effect is thus extremely important in achieving a better understanding of the cavitation phenomenon. The problem is complicated by the interrelations among fluid temperature and pressure and material properties.

The purposes of this investigation were: (1) to determine the effect of increasing ambient pressure on cavitation damage to materials in a vibratory test apparatus; (2) to compare the relative ranking of materials at both high and low pressures, and (3) to investigate some of the metallurgical aspects of cavitation damage.

In conducting this investigation, three materials with widely different mechanical properties were tested in sodium at 800^o F (700^o K)

using a magnetostrictive-type vibratory apparatus. Argon cover gas was used over the liquid sodium to maintain pressures ranging from one to four atmospheres. Cavitation damage was determined by obtaining volume loss measurements and by metallographic studies.

MATERIALS, APPARATUS AND PROCEDURE

Materials

The materials investigated were AISI type 316 stainless steel, and the cobalt-base alloys, L-605 (HS-25) and Stellite 6B. These three materials were chosen because of the wide differences they exhibited to cavitation damage in sodium at atmospheric pressure (ref. 4). Type 316 stainless steel showed low resistance to cavitation damage. L-605 showed intermediate resistance to damage. Stellite 6B was the most resistant alloy. The nominal chemical composition of each alloy is listed in table I. The heat treatments, densities, and mechanical properties are given in table II.

Reactor grade sodium (99.95 percent purity) was used as the test fluid. Chemical analyses indicated an initial oxygen level of less than 10 ppm for the sodium. Purity of the sodium was maintained by the addition of a titanium - sponge hot trap to the liquid metal bath.

Accelerated Cavitation Damage Test Facility

The apparatus used is shown schematically in figure 1. A complete description of the facility and test procedure is given in reference 4. Figure 1 illustrates the vacuum dry box arrangement, magnetostrictive transducer assembly, and separately sealed liquid metal test chamber with associated argon line, vapor trap, and pressure gage. The dry box

and test chamber were evacuated to a pressure of approximately 10^{-3} torr (0.13 N/m^2) and backfilled with high purity argon prior to testing.

The specimen was attached to the end of a resonant system consisting of a transducer, exponential horn, and an extension-rod specimen holder. The amplitude and frequency of vibration were detected by a magnetic pickup, and read on an oscilloscope. An automatic feedback system maintained constant amplitude irrespective of variations in resonant frequency induced by temperature changes.

When the transducer assembly was lowered into position, a sleeve attached to the nodal flange on the amplifying horn sealed the liquid metal test chamber from the dry box, and the test chamber pressure was regulated through a separate argon line. Pressures were measured with a precision pressure gage having an accuracy of $1/4$ of 1 percent.

Test Conditions

The test conditions for each material are listed in table III. All tests were run in sodium at $800 \pm 10^\circ \text{ F}$ (700° K); the vapor pressure of sodium at this temperature is 0.015 psia ($1.03 \times 10^2 \text{ N/m}^2$) (ref. 12). The frequency of vibration of the test specimens was nominally $25\,000 \text{ Hz}$, and the peak to peak displacement amplitude was $0.00175 (\pm 0.00005) \text{ inch}$ ($4.45 \times 10^{-2} \text{ mm}$). The specimen surface was immersed to a depth of approximately 0.13 inch (3.3 mm).

Test Procedure

The type of specimen used is shown in figure 2. The test surface of each specimen was metallographically polished before test to allow meaningful examination of the specimen surface at high magnification

during the early stages of damage. Prior to test the specimens were weighed and photographed. After each period of operation, the specimens were cleaned, weighed and rephotographed. Weight loss measurements were divided by density to obtain volume loss.

Test duration was dependent upon the volume loss rate of each specimen. In most cases, the testing of a specimen was stopped after it maintained a relatively constant volume loss between weighings.

After testing, the specimens were sectioned axially and examined metallographically to determine the depth of cavitation attack and to study any reaction zones that might exist between the sodium and the specimen material.

CAVITATION DAMAGE RESULTS

Cavitation damage, expressed as cumulative volume loss and as volume loss rate is plotted against time for each material tested in figures 3 through 8. The effect of pressure on the rate of cavitation damage is plotted in figures 9 and 10. Cavitation damage data are also summarized in table IV. The results of metallographic studies are presented in figures 11 through 16.

Volume Loss and Volume Loss Rate

The cavitation damage to L-605 at 1, 2, 3, and 4 atmospheres is shown as volume loss in figure 3, and as volume loss rate in figure 4. Volume loss rate curves were obtained by dividing the volume loss between successive weighings by the increment of test time between them. These values were then plotted midway between the weighing times. From figures 3 and 4, it is evident that cavitation at higher pressures results

in: (1) higher cumulative volume loss, (2) a higher volume loss rate peak, and (3) a higher level of steady state volume loss rate. The steady state region is defined in this investigation as the zone of minimum volume loss rate after the damage rate has passed through a peak. In this region the volume loss rate does not change significantly over an extended period of time; and values for a relatively steady-state damage rate can be determined. It is interesting to note that the shape of the rate curve varies with pressure (fig. 4). As the pressure is increased, the peak of the damage rate curve is higher, narrower, and occurs earlier.

During the one atmosphere test the first L-605 specimen tested failed at the threaded joint after 90 minutes exposure. The test was repeated with a second specimen and continued for 360 minutes. Damage was slight during the first 90 minutes, and the data were virtually identical for the two specimens. Consequently, one smooth curve was drawn through the data. At 3 atmospheres, a similar specimen failure occurred after 120 minutes. A second specimen was therefore run and the test continued for a total 360 minutes. Because the cumulative volume loss of the two specimens run at the same pressure showed a difference of about 10 cubic millimeters at the 120 minute point, separate curves are plotted in figures 3 and 4.

Figure 4 shows that the volume loss rate curves increase for the specimens tested at 3 and 4 atmospheres after 240 minutes. This increase is most likely due to undercutting of the surface by cavitation and the resultant loss of large particles of material. Some large particles of specimen material were found in the sodium bath. Further evidence of

such undercutting is presented in the section dealing with the metallographic studies.

Volume loss and volume loss rate curves are shown in figures 5 and 6, respectively, for type 316 stainless steel at 1, 2.7, and 4 atmospheres. Similar curves for Stellite 6B are shown in figures 7 and 8. Increasing the test pressure increased the cumulative volume loss in each case and both materials exhibited steady state volume loss rates that increased with increasing pressure. However, the volume loss rate peaks were not as well defined as for the L-605 specimens (fig. 4).

The effect of pressure on the volume loss of the Stellite 6B specimens was not as clearly defined as in the case of the other materials. There is relatively little spread between the 2.7 and 4 atmosphere test results. The unusual behavior of this material may be due in part to the changing patterns of the damage. This will be discussed further in the section on metallography. Although there is an overlap of the rate curves for Stellite 6B (fig. 8), the peak damage rate and steady state damage rate increase with increasing test pressure.

Relation Between Steady State Volume Loss Rate and Pressure

The steady state volume loss rates for L-605, 316 stainless steel and Stellite 6B determined from figures 4, 6, and 8, respectively, are listed in table IV. These values are plotted against pressure in figure 9. Assuming that cavitation damage can be expressed by the steady state volume loss rate of a material, damage increases linearly with ambient pressure for the pressure range considered. Of course, under other test conditions (different amplitudes of vibration, temperature, specimen size,

etc.) this relation might not hold true. It is important to note that the resulting linear relation is based upon the conventional method of measuring cavitation damage which does not take into account the damage pattern.

From the photographs of figures 11 to 15, it is obvious that there is an area of heavy damage, and a surrounding area of little or no damage on the tested specimens. The heavily damaged area was reduced in size but its depth increased as the cover gas pressure was increased. If the volume loss rate data are normalized on the basis of damaged area only, the effect of pressure on volume loss rate will no longer be linear but volume loss rate will vary as a power of pressure. The normalized cavitation damage data are listed in table V and plotted in figure 10. In figure 10, the slopes of the curves for 316 stainless steel, L-605, and Stellite 6B are 2.0, 2.2, and 2.7, respectively.

The results of the present investigation differ from those obtained by previous investigators (ref. 11). Using a low frequency (6500 Hz) magnetostrictive device in water, they found that for a given exposure time, damage increased with increasing pressure up to about 2 atmospheres and subsequently decreased as pressure was further increased. No damage was observed at 4 atmospheres. We believe that because the apparatus used for the earlier tests (ref. 11) had a relatively low frequency resulting in relatively low fluid velocities, cavitation was reduced at the higher pressures. The high frequency device used in the present investigation is capable of generating more cavitation at the

higher fluid pressures.

From figures 9 and 10, it is also apparent that materials have the same relative ranking with respect to cavitation damage resistance at high pressures that they have at atmospheric pressure. Accelerated material damage tests, therefore, may be run at higher ambient pressures, and test time can be shortened by at least an order of magnitude.

A 316 stainless steel specimen was run for a test time of 16 hours at 0.5 atmosphere. During the last 8 hours of this test, the specimen had a steady state damage rate of approximately 0.5 cubic millimeter per hour. This value is also plotted on figure 9. It is believed that a zero damage rate occurs when cover gas pressure is very near the vapor pressure of the fluid.

It can be observed from figure 9 that the curves for more severely damaged materials have the steeper slopes; and it would appear that the relative effect of pressure on the damage rate is greater for the less resistant materials. If, however, the data are normalized (fig. 10), this trend is reversed; that is, the curves of the more resistant materials have steeper slopes and the relative effect of pressure on the damage rate is greater for the more resistant materials.

Metallography

Macrographs were taken of all the specimens tested. The damaged surfaces of L-605 specimens are illustrated in figure 11. After only 15 minutes severe damage is evident in specimens exposed at 4 atmospheres, whereas the specimens exposed at 1 atmosphere show very little damage even after 60 minutes of testing. Several large projections can

be seen in the central portion of the surfaces of specimens exposed for 360 minutes at 3 and 4 atmospheres. Undercutting and loss of such projections are believed to be the reason the volume loss rate curves (fig. 4) showed an increase at the longer exposure times. Evidence of undercutting is apparent in the macrographs of figure 12. This figure clearly shows the increasing depth and amount of attack with increasing pressure. Wider undamaged rims and greater undercutting are evident in the specimens tested at higher pressures. Calculated areas of heavy damage are shown in table V.

Damaged surfaces of 316 stainless steel and Stellite 6B specimens are shown in figures 13 and 14, respectively. As in the case of L-605, damage at 4 atmospheres was much more severe than that at 1 atmosphere, and damage was primarily concentrated in the central region of the specimens. The 316 stainless steel specimen sustained such severe attack at 4 atmospheres that even portions of the rim were damaged. Although not shown, the heavily damaged specimens of 316 stainless steel and Stellite 6B were also sectioned and macrographs were taken. These had a similar appearance to the sectioned L-605 specimens shown in figure 12.

Photomicrographs were taken of the surfaces of the L-605 specimens in the early stages of cavitation attack. These together with the original microstructure of a L-605 specimen are shown in figure 15. The specimen was electrolytically etched with a solution of HCl (30 ml) and H_2O_2 (3 drops), and was repolished before testing. Specimens tested at pressures above 2 atmospheres were damaged too severely to show significant

features under high magnification. In all cases during the early stages of damage, attack along grain and twin boundaries was noted.

Figure 16 shows photomicrographs of sectioned specimens of all materials before and after testing. All of the materials tested exhibited gross undercutting and transgranular cracking. Evidence of sub-surface deformation existed in the form of slip bands for all materials. Bending of twin boundaries was observed in L-605 (fig. 16(a)). Breaking of sub-surface carbides in Stellite 6B is apparent in figure 16(c). No evidence of any reaction zone was found in the cavitation damaged regions of any specimen.

Comparison of Accelerated Cavitation Damage and Pump Impeller Test Results

An interesting example of the effect of pressure on cavitation damage to a pump impeller operated in a liquid metal has been reported in reference 1. In this investigation an impeller of 316 stainless steel was operated first in water at room temperature then in potassium at 1400° F (1033° K). Photographs were taken of the cavitation cloud formations near the impeller vanes during operation in water at various pump inlet pressures and flow conditions. From these photographs (figs. 26 through 30, ref. 1) it can be seen that, in general, extensive cavitation cloud formations occurred in the low pressure regions near the inlet. Higher pressure regions showed considerably less cavitation.

After the impeller was run in potassium at 1400° F (1033° K) for 350 hours, impeller vanes were examined for cavitation damage. Severe vane damage occurred in the region of higher pressure while little or no damage was noted near the inlet where lower pressures were encountered.

These results indicate that cavitation bubbles collapsing in a high pressure region cause much more damage than bubbles that collapse in a lower pressure region. Thus, observations made in an actual pump application agree qualitatively with the results of our accelerated tests.

SUMMARY OF RESULTS

The effect of pressure on the resistance to cavitation damage of candidate materials for components of liquid metal space power conversion systems was investigated. A vibratory apparatus was used. Three materials, L-605, Stellite 6B, and 316 stainless steel were subjected to accelerated cavitation damage in 800^o F (700^o K) sodium under cover gas pressures of 1 to 4 atmospheres. The following results were obtained:

1. Increasing cover gas pressure significantly increased cavitation damage to all materials. For example, an L-605 specimen tested under one atmosphere pressure for 360 minutes exhibited a volume loss of 10 cubic millimeters, as compared to 200 cubic millimeters after 360 minutes under 4 atmospheres. This result implies that in fluid systems where cavitation occurs in high pressure regions, damage to components may be much greater than would normally be expected from cavitation tests conducted at atmospheric pressures.

2. Within the range of conditions (specimen size and cover gas pressures) considered in this investigation, the steady state volume loss rate (based upon total specimen area) for each material increased linearly with cover gas pressure. When the volume loss rate data were

normalized to include only the heavily damaged area of the specimens, the steady state volume loss rate increased exponentially from 2.0 to 2.7 power of pressure.

3. The relative ranking of the materials with respect to resistance to cavitation damage was the same regardless of cover gas pressure. (It was, in order of increasing damage - Stellite 6B, L-605 and 316 stainless steel.) This result together with the fact that the damage rate increases with increasing pressure suggests that a greater number of materials may be evaluated in a given time at higher pressures than at atmospheric pressure.

4. Metallographic examination of axially sectioned specimens of all the materials tested revealed severe undercutting of the surface and transgranular cracking. Subsurface deformation was indicated in all materials by the appearance of slip bands. Stellite 6B showed extensive cracking of carbides beneath the surface, and L-605 exhibited some bending of twins near the surface.

Lewis Research Center,
National Aeronautics and Space Administration,
Cleveland, Ohio.

slk - 5/15/67

REFERENCES

1. Kulp, Robert S.; and Altieri, James V.: Cavitation Damage of Mechanical Pump Impellers Operating in Liquid Metal Space Power Loops. Pratt and Whitney Aircraft (NASA CR-165), 1965.
2. Smith, P. G.; DeVan, J. H.; and Grindell, A. G.: Cavitation Damage to Centrifugal Pump Impellers During Operation with Liquid Metals and Molten Salt at 1050^o to 1400^o F. J. Basic Eng., vol. 85, no. 3, Sept. 1963, pp. 329-335; Discussion pp. 335-337.
3. Hammitt, F. G.: Observations on Cavitation Damage in a Flowing System. J. Basic Eng., vol. 85, no. 3, Sept. 1963, pp. 347-359.
4. Young, S. G.; and Johnston, J. R.: Accelerated Cavitation Damage of Steels and Superalloys in Liquid Metals. NASA TN D-3426, May 1966.
5. Garcia, R.; Hammitt, F. G.; and Nystrom, R. E.: Comprehensive Cavitation Damage Data for Water, Mercury, and Lead-Bismuth Alloy Including Correlations with Material and Fluid Properties. (ASTM STP-408.) Paper No. 122, 69th Annual Meeting of the ASTM, Atlantic City, N. J., June 24-July 1, 1966.
6. Thiruvengadam, A.; and Preiser, H. S.: Cavitation Damage in Liquid Metals. Report no. TR 467-Final, Hydronautics, Inc. (NASA CR-72035), Nov. 1965.
7. Knapp, Robert T.: Recent Investigations of the Mechanics of Cavitation and Cavitation Damage. Trans. ASME, vol. 77, no. 7, Oct. 1955, pp. 1045-1054.

8. Plesset, M. S.; and Ellis, A. T.: On the Mechanism of Cavitation Damage. Trans. ASME, vol. 77, no. 7, Oct. 1955, pp. 1055-1064.
9. Naude, Charl F.; and Ellis, Albert T.: On the Mechanism of Cavitation Damage by Non-Hemispherical Cavities Collapsing in Contact with a Solid Boundary. J. Basic Eng., vol. 83, no. 4, Dec. 1961, pp. 648-656.
10. Knapp, R. T.; and Hollander, A.: Laboratory Investigations of the Mechanism of Cavitation. Trans. ASME, vol. 70, no. 5, July 1948, pp. 419-431; Discussion, pp. 431-435.
11. Peters, H.; and Rightmire, B. G.: Cavitation Study by the Vibratory Method. Proceedings, Fifth International Cong. for Applied Mechanics, 1938, pp. 614-616.
12. Weatherford, W. D., Jr.; Tyler, John C.; and Ku, P. M.: Properties of Inorganic Working Fluids and Coolants for Space Applications. WADC Technical Report 59-598, Dec. 1959.

TABLE I. - NOMINAL CHEMICAL COMPOSITIONS OF TEST MATERIALS

Material	Composition, weight percent											
	Iron	Nickel	Cobalt	Chromium	Molybdenum	Tungsten	Carbon	Manganese	Silicon	Phosphorus	Sulfur	Copper
Stellite 6B ^b	a 3	a 3	Bal.	30	a 1.5	4.5	1.1	a 2	a 2	-----	-----	-----
L-605 AMS 5759B ^c	a 3	10	Bal.	20	-----	15	0.1	1.5	a 1.0	a 0.04	a 0.03	-----
AISI 316 stainless steel AMS 5648C ^c	Bal.	13	---	18	2.5	----	0.08	1.6	a 1.0	a 0.04	a 0.03	a 0.50

^aMaximum.

^bAnon.: Wear Resistant Alloys, Bulletin no. F30-1-33-A, Haynes Stellite Co., 1962.

^cAerospace Materials specifications.

TABLE II. - HEAT TREATMENTS, DENSITIES, AND 800° F (700° K) MECHANICAL PROPERTIES OF TESTING MATERIALS

PROPERTIES OF TESTING MATERIALS

Material	Heat treatment	Density	Ultimate tensile strength	Yield strength (0.2 percent offset)	Elongation, percent
Stellite 6B ^a	Solution-heat treated at 2250° F (1506° K); air cooled	0.303 lb/in. ³ (8.38 × 10 ³ kg/m ³)	138 000 psi (9.52 × 10 ⁸ N/m ²)	71 000 psi (4.90 × 10 ⁸ N/m ²)	29.0
L-605 ^b	Solution-heat treated at 2250° F (1506° K); water quenched	0.330 lb/in. ³ (9.13 × 10 ³ kg/m ³)	119 000 psi (8.21 × 10 ⁸ N/m ²)	35 000 psi (2.42 × 10 ⁸ N/m ²)	75.0
AISI 316 ^b stainless steel	Annealed	0.288 lb/in. ³ (7.98 × 10 ³ kg/m ³)	70 000 psi (4.82 × 10 ⁸ N/m ²)	28 000 psi (1.93 × 10 ⁸ N/m ²)	40.0

^a Anon.: Wear Resistant Alloys. Bulletin no. F30-1-33A. Haynes Stellite Co., 1962.

^b V. Weiss and J. G. Sessler, eds.: Aerospace Structural Metals Handbook. Syracuse University Press, 1966.

TABLE III. - TEST CONDITIONS

[Temperature, $800 \pm 10^{\circ}$ F (700° K); fluid, sodium (99.95 percent purity); frequency, $25\,000 \pm 500$ Hz; amplitude, 0.00175 ± 0.00005 inch (4.45×10^{-2} mm).]

Material	Pressure, ^a atm	Total test time, min
Stellite 6B	1.0	600
Stellite 6B	2.7	540
Stellite 6B	4.0	480
L-605	1.0	360
L-605	2.0	360
L-605	3.0	360
L-605	4.0	360
316 stainless steel	1.0	240
316 stainless steel	2.7	300
316 stainless steel	4.0	240

^aNominal pressure, ± 0.02 atmosphere (1 atmosphere = 1.01×10^5 N/m²).

TABLE IV. - SUMMARY OF CAVITATION TEST DATA

Material	Cover gas pressure, atm	Volume loss, mm ³											Steady state volume loss rate, mm ³ /hr
		Time, min											
		60	120	180	240	300	360	420	480	540	600		
Stellite 6B	1.0	----	(0.04)	(0.13)	0.4	1.1	1.6	2.1	2.6	----	3.6	0.5	
Stellite 6B	2.7	----	16.8	27.0	39.0	49.2	54.8	60.1	65.5	69.8	----	5.0	
Stellite 6B	4.0	17.1	29.0	36.1	43.3	51.7	62.1	----	80.6	----	----	7.2	
L-605	1.0	0.1	1.0	3.0	5.0	7.5	10.0	----	----	----	----	2.4	
L-605	2.0	8.7	25.3	38.8	48.3	59.3	70.9	----	----	----	----	10.5	
L-605-(1)	3.0	27.1	49.9	----	----	----	----	----	----	----	----	----	
L-605-(2)	3.0	----	61.3	79.1	95.5	113	141	----	----	----	----	17.7	
L-605	4.0	46.6	74.5	102	130	160	201	----	----	----	----	27.5	
316 stainless steel	1.0	3.6	8.6	13.8	18.0	----	----	----	----	----	----	4.2	
316 stainless steel	2.7	----	63.3	90.8	119	153	----	----	----	----	----	27.2	
316 stainless steel	4.0	71.0	124	165	209	----	----	----	----	----	----	41.0	

VOLUME LOSS RATE

Material	Pressure, atm	Heavy damage area, ^a mm ²	Normalizing factors ^b	Normalized steady state volume loss rate, ^c mm ³ /hr
Stellite 6B	1.0	140	1.2	0.6
Stellite 6B	2.7	96	1.7	8.5
Stellite 6B	4.0	45	3.6	26
L-605	1.0	150	1.1	2.6
L-605	2.0	140	1.2	13
L-605	3.0	99	1.6	28
L-605	4.0	80	2.0	55
316 stainless steel	1.0	130	1.2	5.2
316 stainless steel	2.7	96	1.7	46
316 stainless steel	4.0	74	2.2	90

^a(Average diameter of damaged area)² × π/4.

^bArea of undamaged specimen/heavy damaged area.

^cSteady state volume loss rate (from table IV) × normalizing factor.

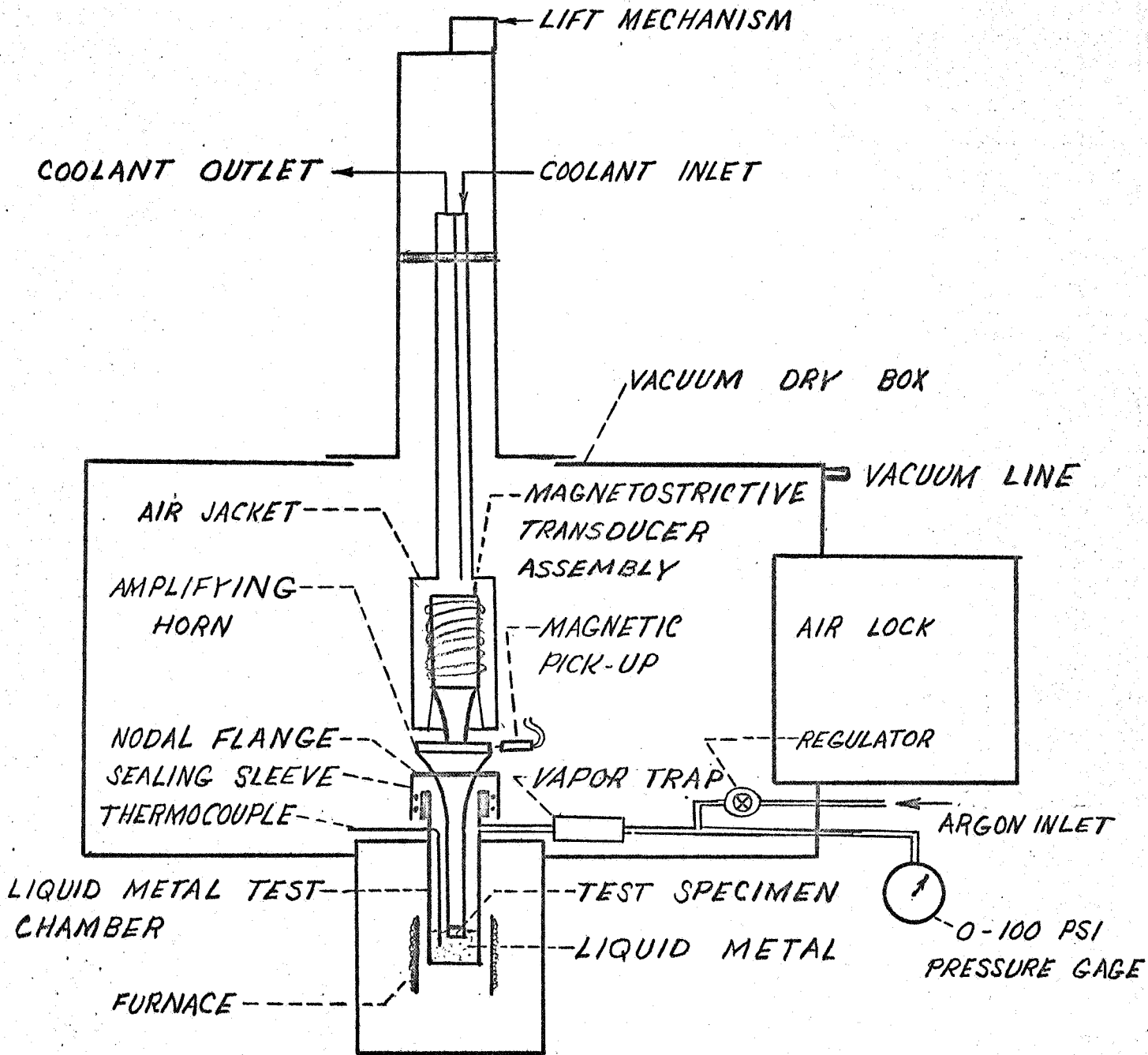


FIGURE 1. - SCHEMATIC DIAGRAM OF CAVITATION APPARATUS

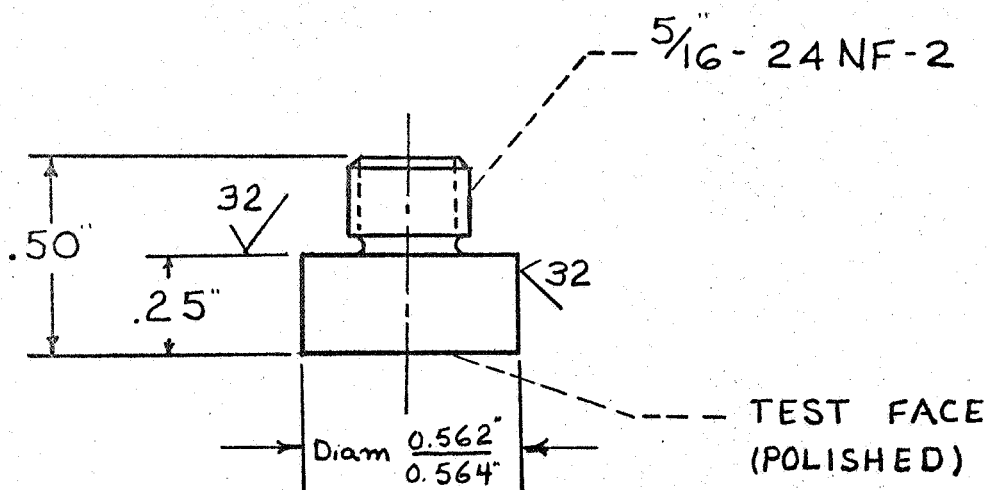


FIGURE 2 . CAVITATION TEST SPECIMEN

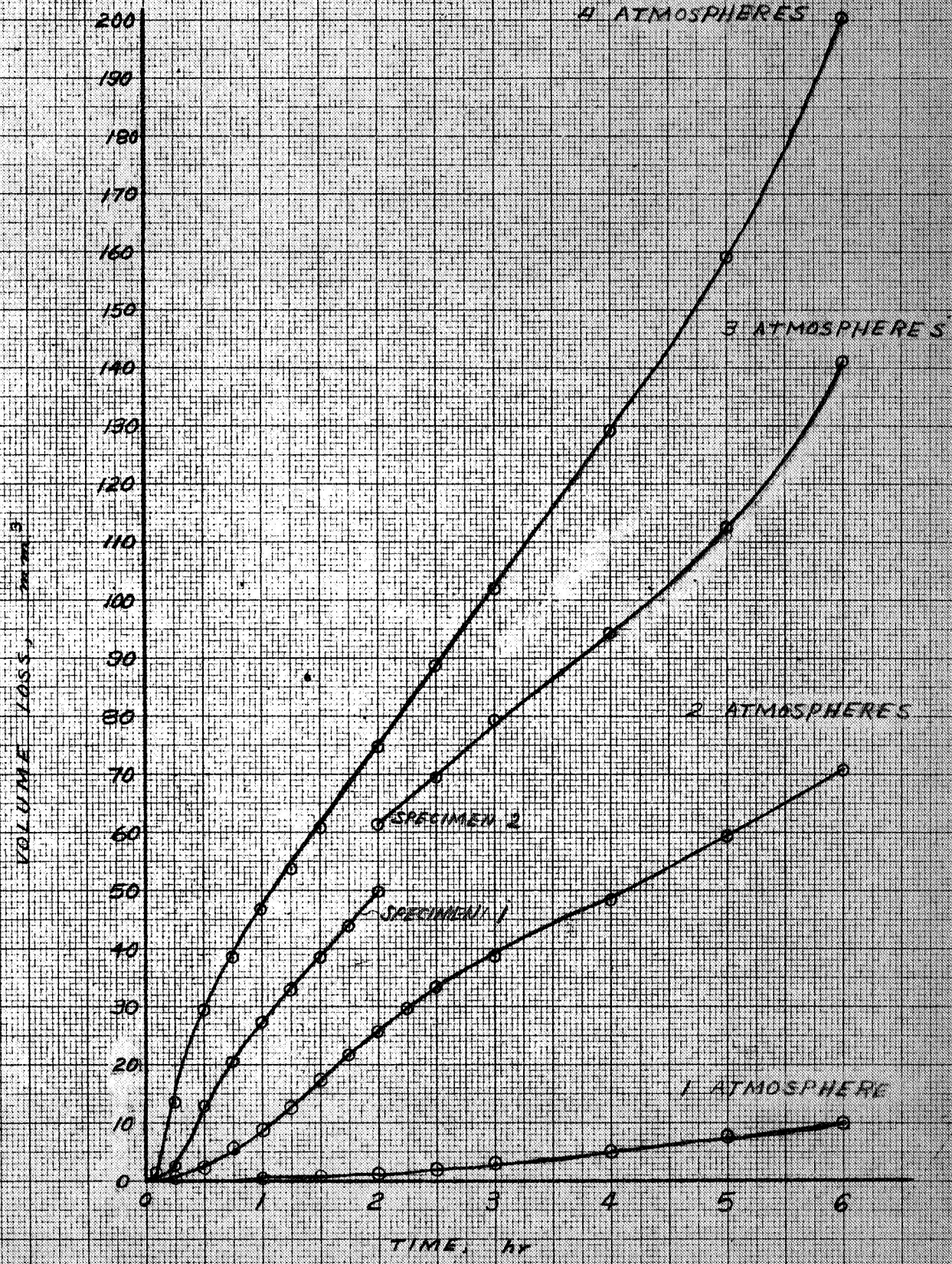


FIGURE 3-CAVITATION DAMAGE OF L-605 IN 800°F SODIUM AT VARIOUS PRESSURES

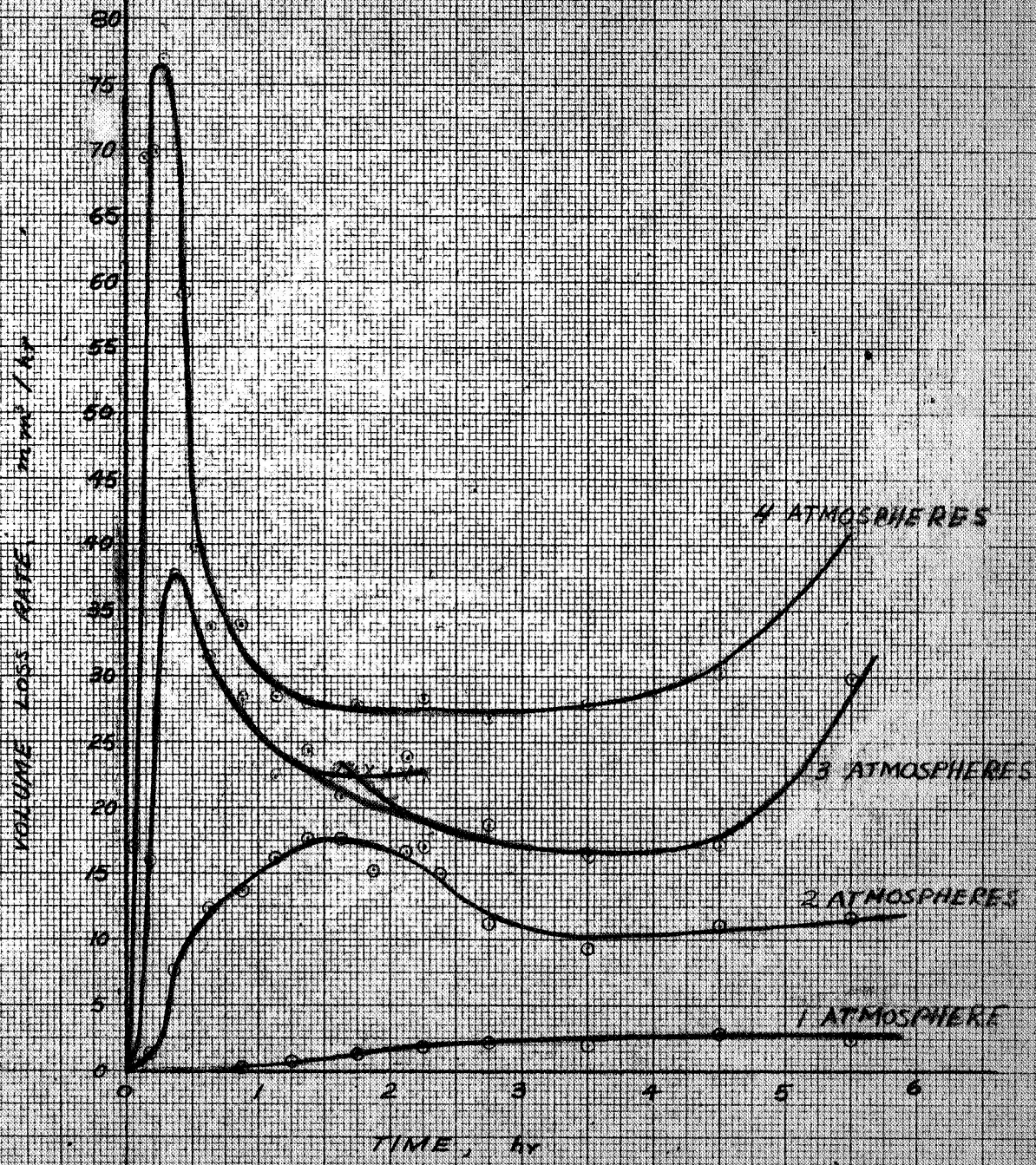


FIGURE 4-RATE OF CAVITATION DAMAGE OF 1.605 IN 800°F SODIUM AT VARIOUS PRESSURES

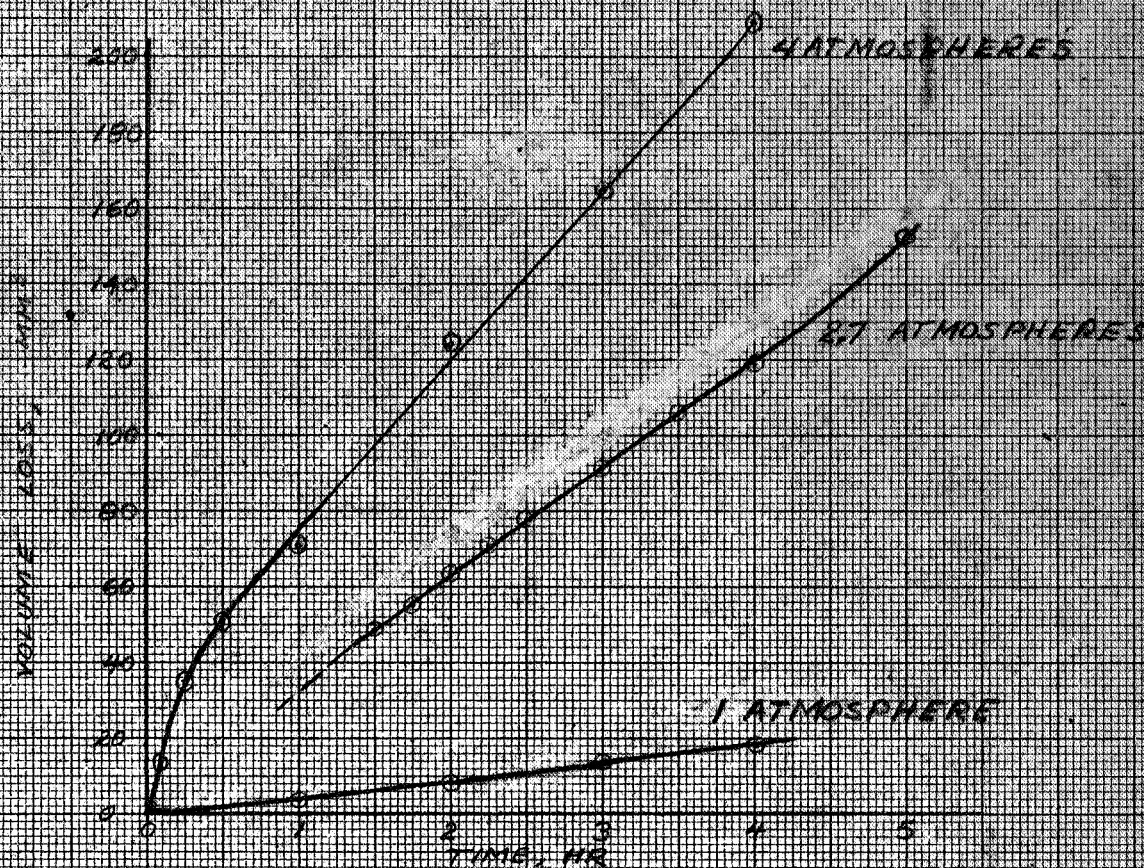


FIGURE 5- CAVITATION DAMAGE OF AISI TYPE 316 STAINLESS STEEL IN 800°F SODIUM AT VARIOUS PRESSURES

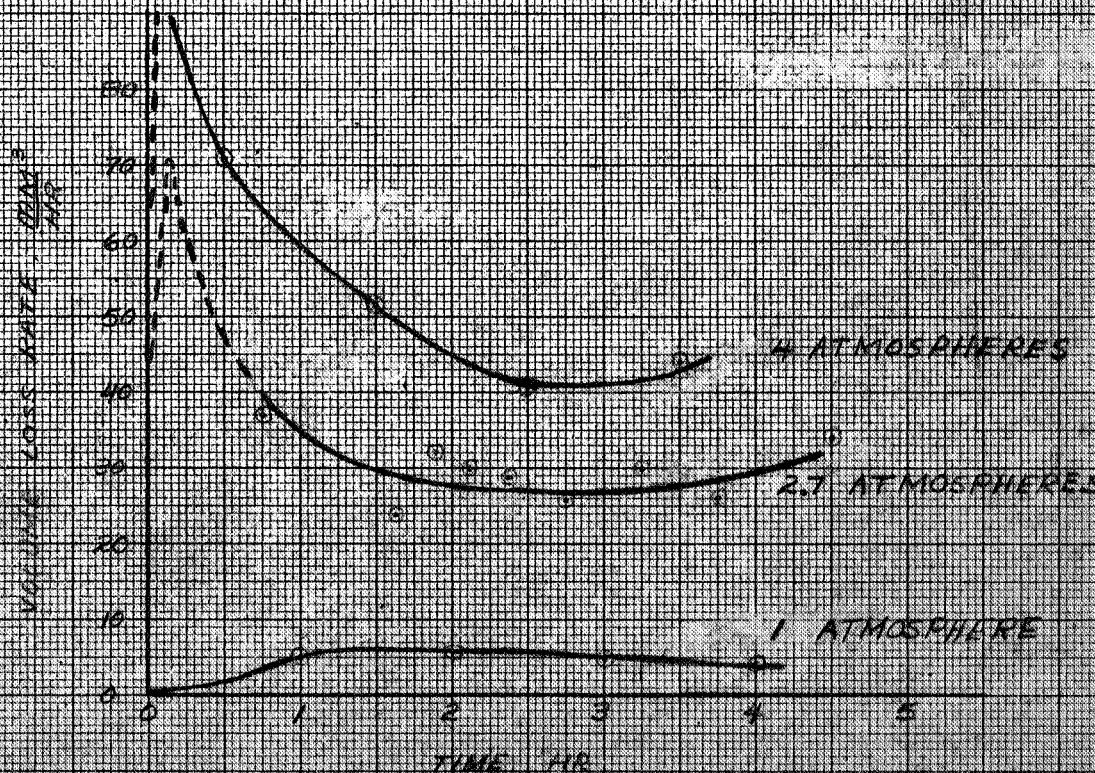


FIGURE 6- RATE OF CAVITATION DAMAGE OF AISI TYPE 316 STAINLESS STEEL IN 800°F SODIUM AT VARIOUS PRESSURES

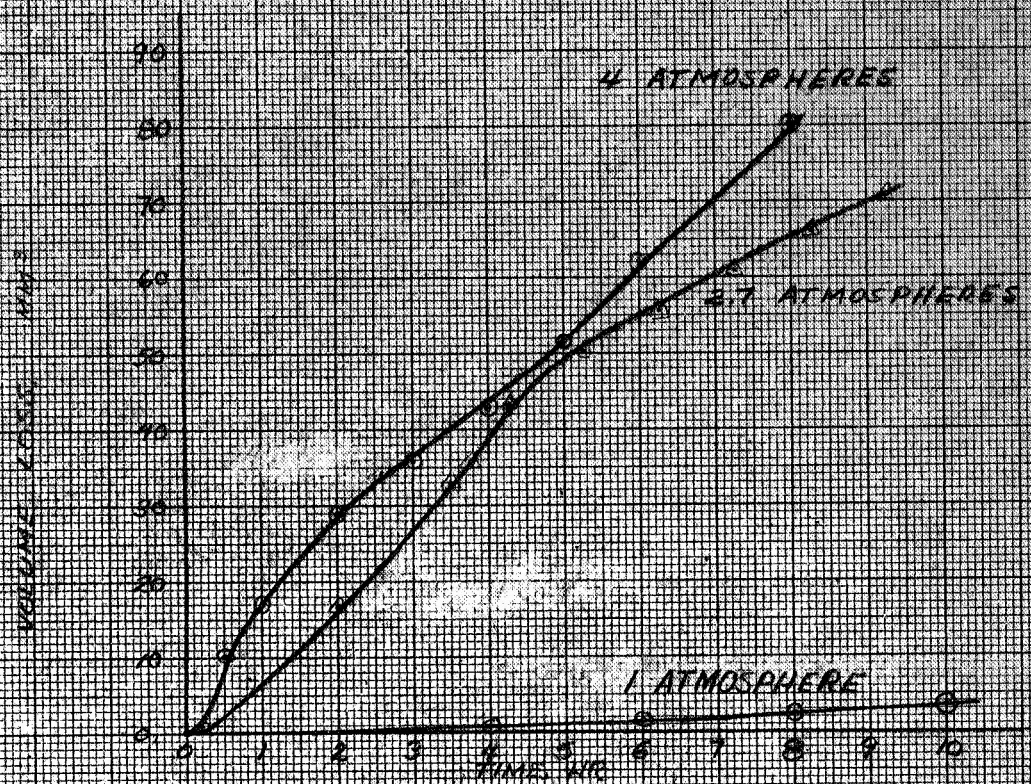


FIGURE 7 - CAVITATION DAMAGE OF STELLITE 6B IN 800°F SODIUM AT VARIOUS PRESSURES

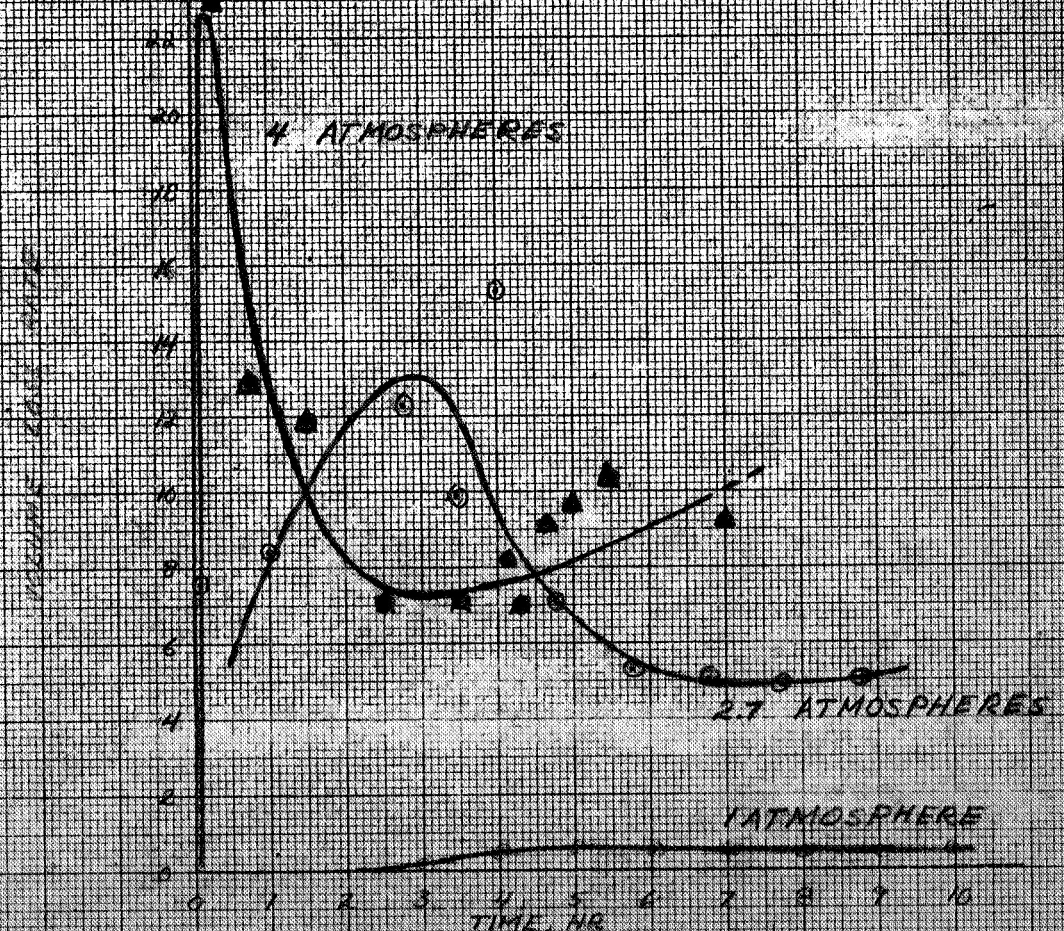


FIGURE 8 - RATE OF CAVITATION DAMAGE OF STELLITE 6B IN 800°F SODIUM AT VARIOUS PRESSURES.

STEADY STATE VOLUME LOSS RATE, MM³/HR

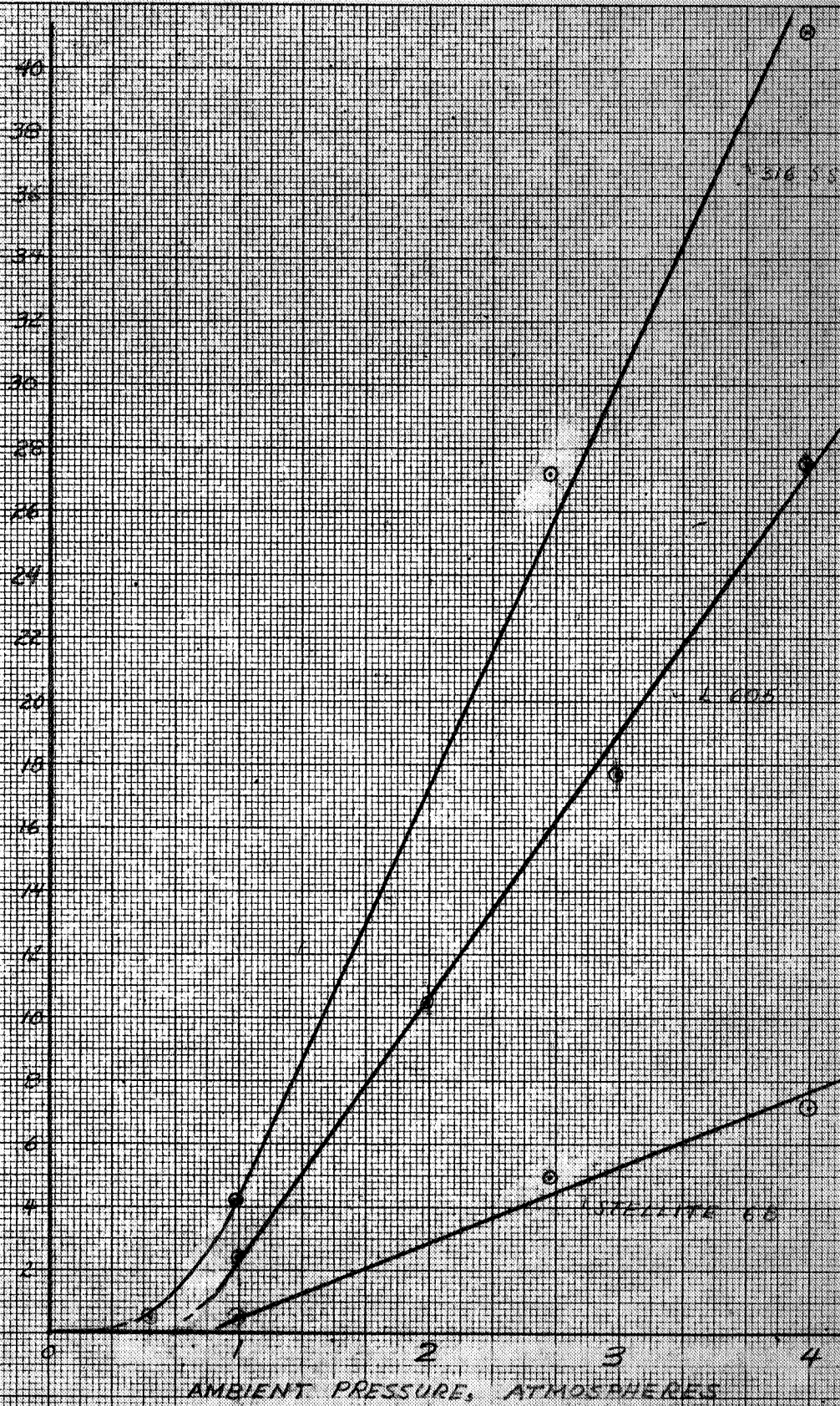


FIGURE 9 : RELATION BETWEEN CAVITATION DAMAGE RATE AND AMBIENT PRESSURE FOR MATERIALS TESTED IN 800° F SODIUM

NORMALIZED STEADY STATE VOLUME LOSS RATE,
MM³ / HR

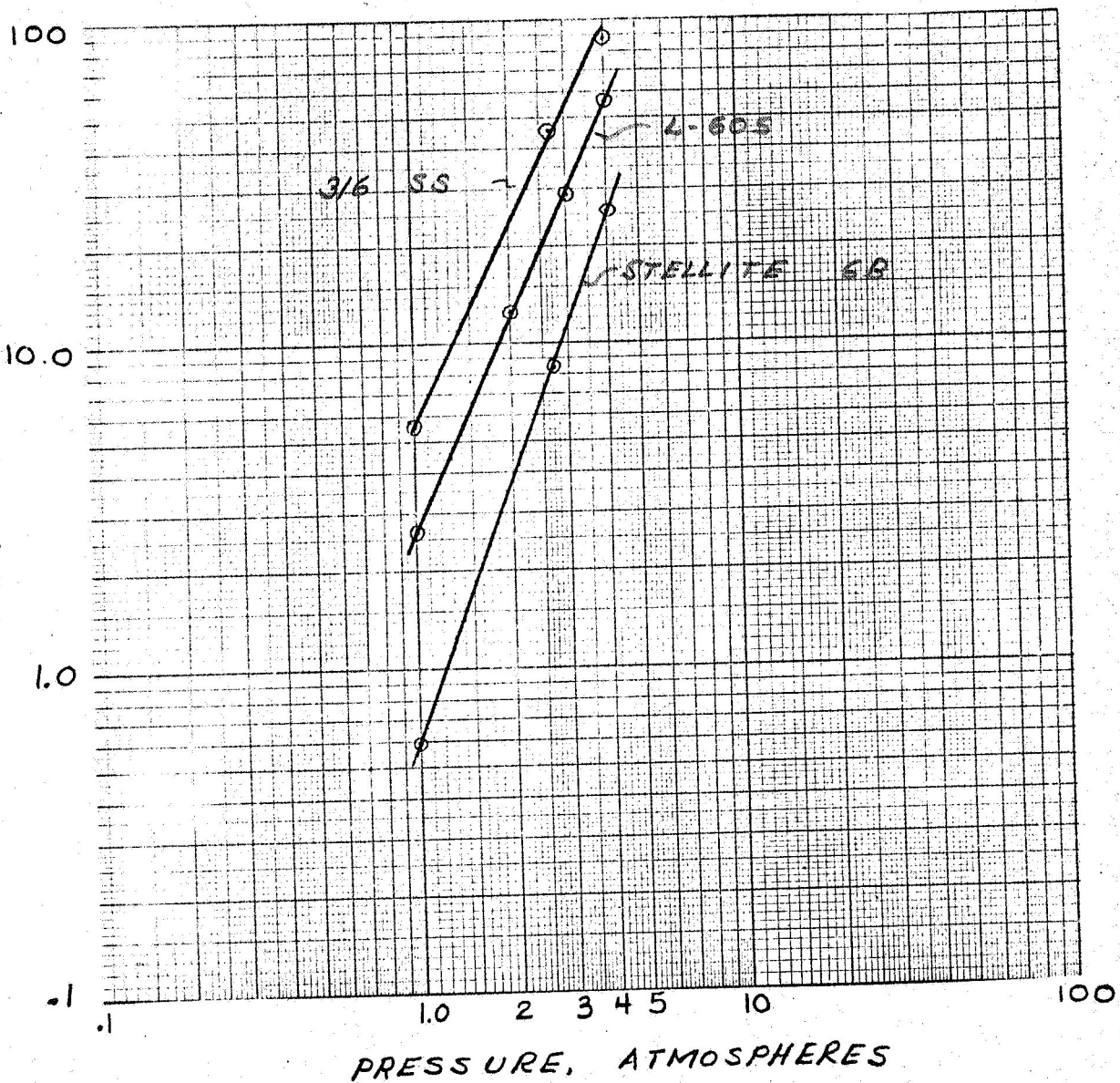
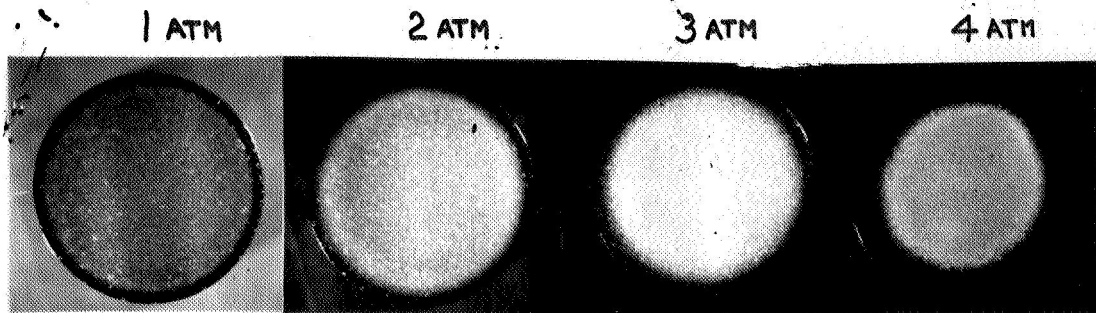
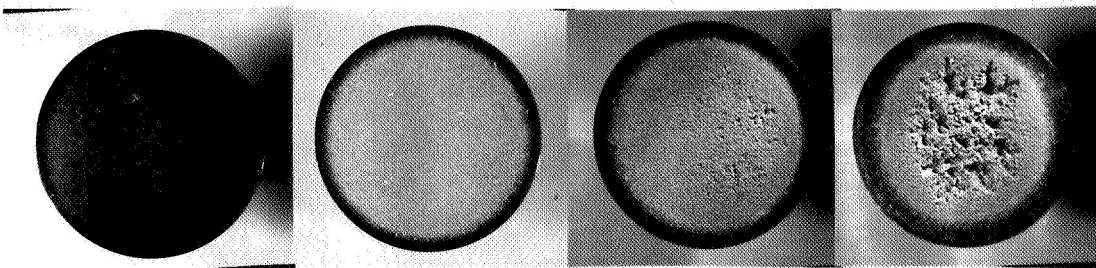


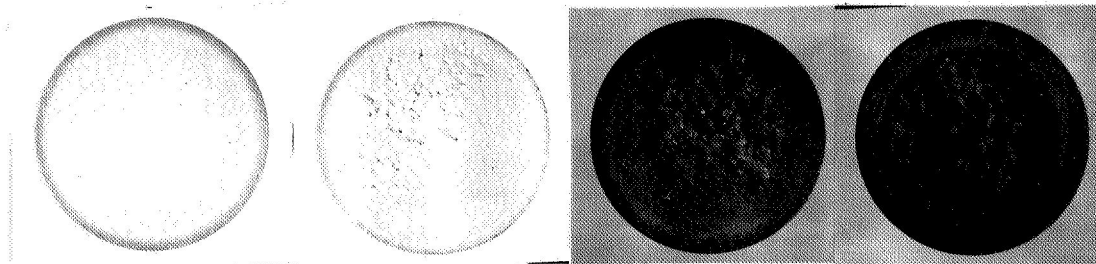
FIGURE 10 - RELATION OF CAVITATION DAMAGE, NORMALIZED TO AN AREA BASIS, TO AMBIENT PRESSURE FOR MATERIALS TESTED IN 800° F SODIUM.



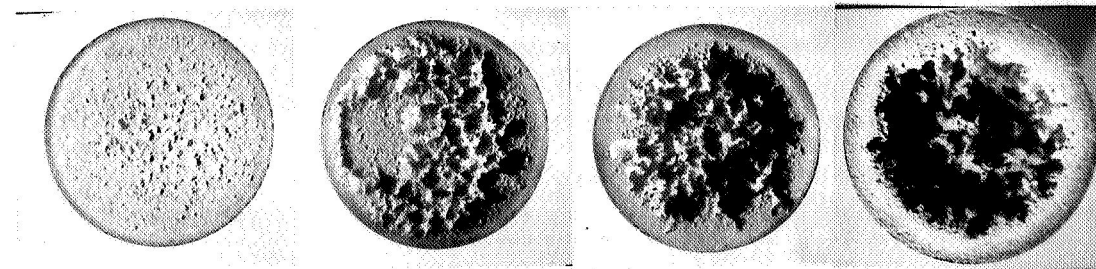
5 MIN.



15 MIN.

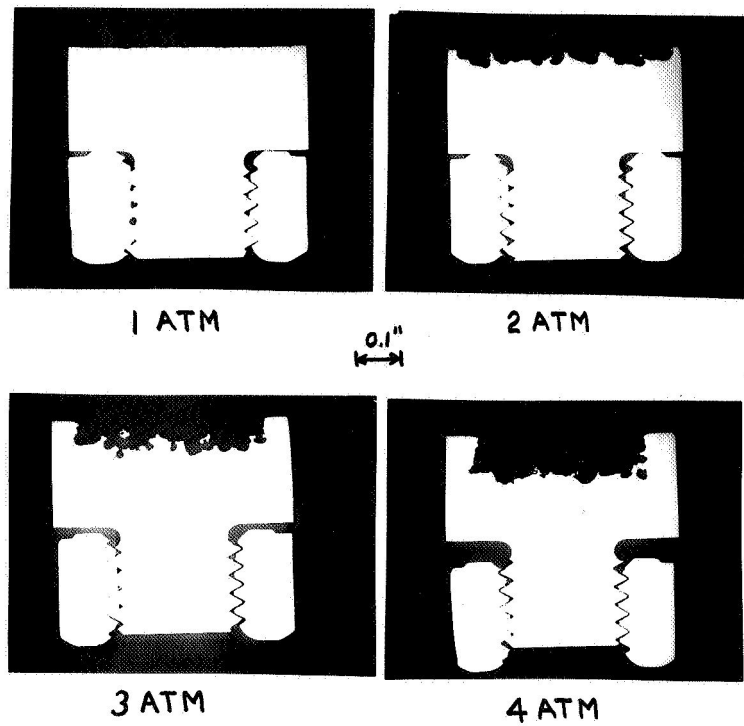


60 MIN.



360 MIN.

II
 FIG. 0 - DAMAGED SURFACES OF L-605 SPECIMENS AFTER EXPOSURE TO CAVITATION IN SODIUM AT 800°F AT VARIOUS TIMES AND PRESSURES.



12
FIGURE 12 - SECTIONS OF L-605 SPECIMENS
AFTER EXPOSURE TO CAVITATION IN SODIUM AT
800°F FOR 6 HOURS AT VARIOUS PRESSURES.
(UNETCHED)

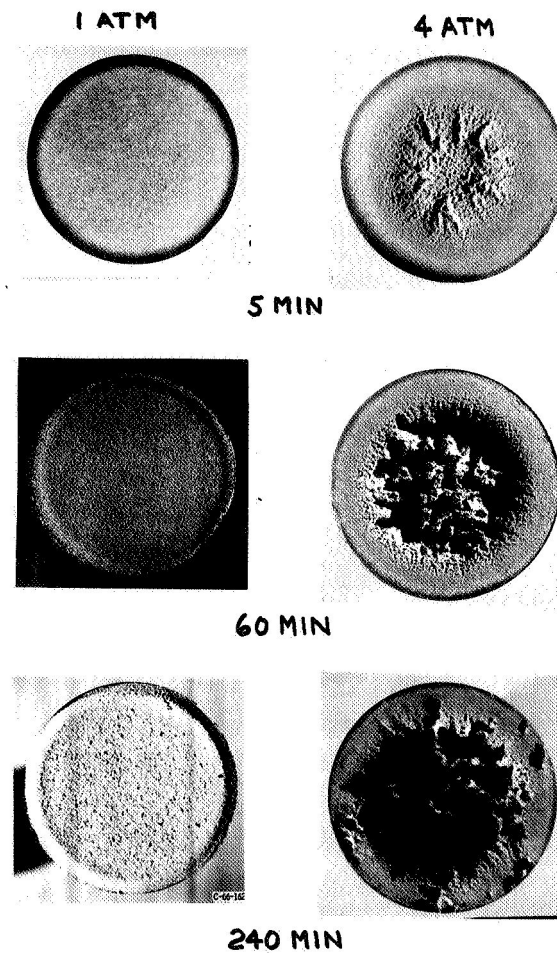
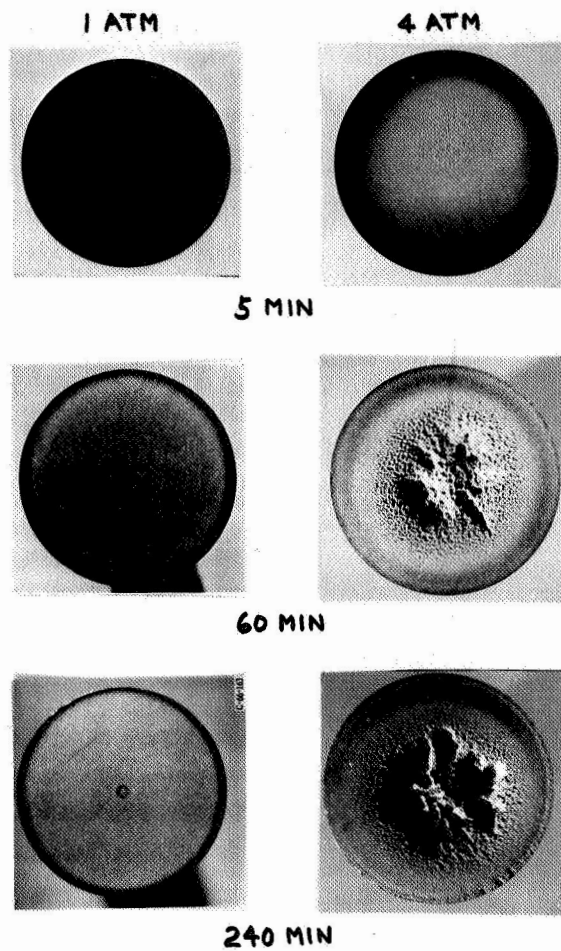
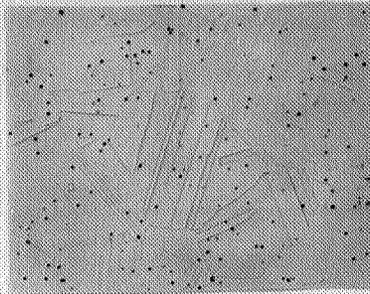


FIGURE 13- DAMAGED SURFACES OF AISI 316
STAINLESS STEEL SPECIMENS AFTER EXPOSURE
TO CAVITATION IN SODIUM AT 800°F AT VARIOUS
TIMES AND PRESSURES.

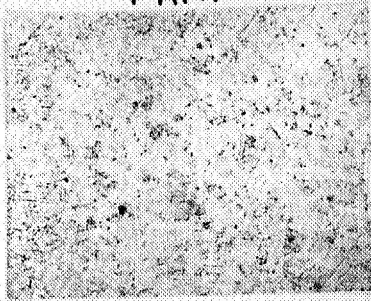


**FIGURE 14- DAMAGED SURFACES OF STELLITE 6B
SPECIMENS AFTER EXPOSURE TO CAVITATION IN
SODIUM AT 800°F AT VARIOUS TIMES AND PRESSURES**

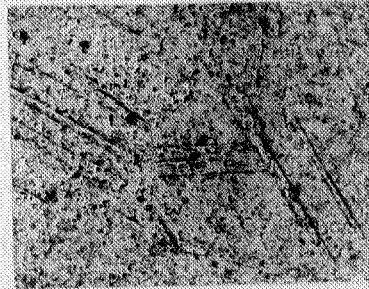


UNTESTED - ETCHED

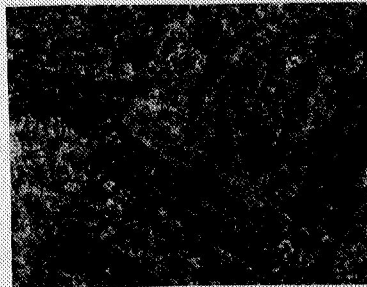
1 ATM



2 ATM

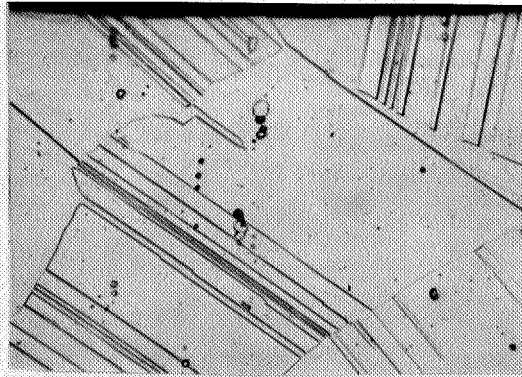


5 MIN

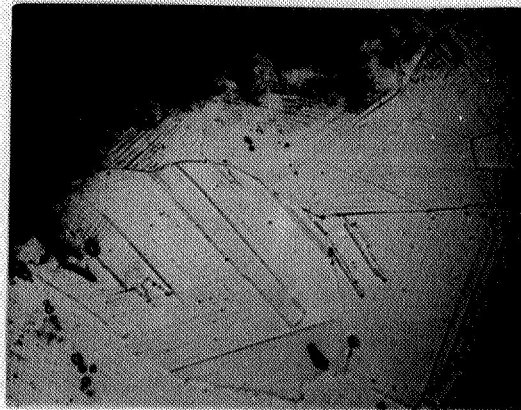


15 MIN

15
FIGURE 15 - PHOTOMICROGRAPHS OF DAMAGED SURFACES OF
L-605 SPECIMENS EXPOSED TO CAVITATION IN SODIUM
AT 800°F. X250.

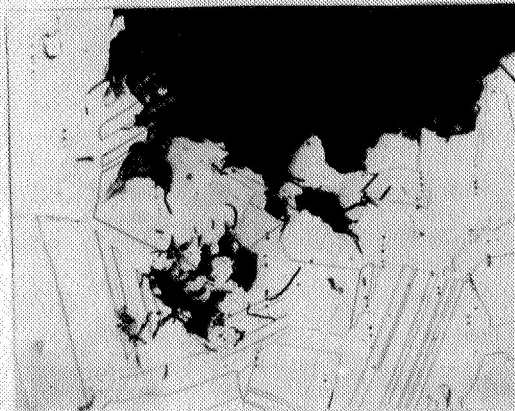


AS RECEIVED 500 X



500 X

**360 MINUTE EXPOSURE AT ONE
ATMOSPHERE**



250 X

**360 MINUTE EXPOSURE AT FOUR
ATMOSPHERES**

(a) L - 605

**FIGURE 16. - PHOTOMICROGRAPHS OF
SECTIONED SPECIMENS EXPOSED TO
CAVITATION IN SODIUM AT 800° F.**



AS RECEIVED

500x



**240 MINUTE EXPOSURE AT ONE
ATMOSPHERE**

500x



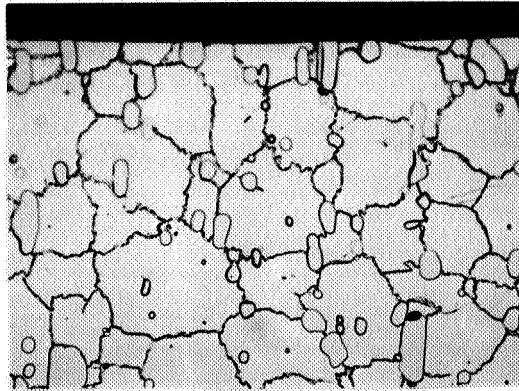
**240 MINUTE EXPOSURE AT FOUR
ATMOSPHERES**

500x

(b) 316 STAINLESS STEEL

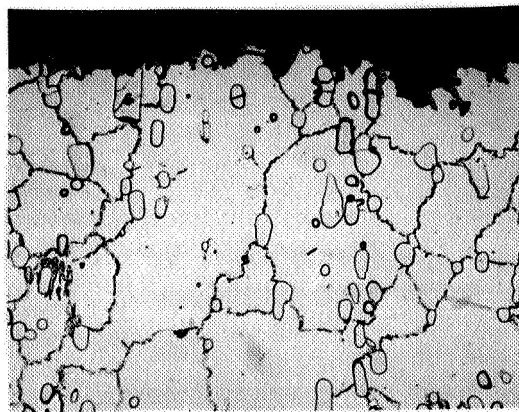
FIGURE 16. - CONTINUED

7



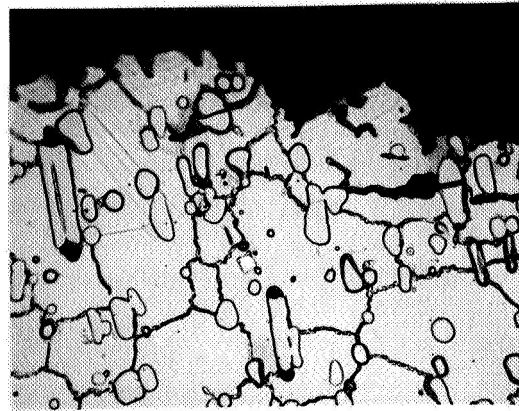
500 x

AS RECEIVED



500 x

600 MINUTE EXPOSURE AT ONE
ATMOSPHERE



500 x

480 MINUTE EXPOSURE AT FOUR
ATMOSPHERES

(c) STELLITE 6B

FIGURE 16. - CONCLUDED